

Dynamic tracking of stem cells in an acute liver failure model

Tarek Ezzat, Dipok Kumar Dhar, Massimo Malago, Steven WM Olde Damink

Tarek Ezzat, Dipok Kumar Dhar, Massimo Malago, Steven WM Olde Damink, HPB and Liver Transplantation Surgery, Royal Free Hospital, University College London, London NW3 2PF, United Kingdom

Tarek Ezzat, Department of Surgery, University of Alexandria, Alexandria, PO Box 21131, Egypt

Steven WM Olde Damink, Department of Surgery, Maastricht University Medical Centre, and Nutrition and Toxicology Research Institute, Maastricht University, Maastricht, PO Box 5800, The Netherlands

Author contributions: Ezzat T participated in the study design, performed the majority of the experiment, analyzed and interpreted the data, and wrote the first draft of the article; Dhar DK participated in the study design, analyzed and interpreted the data, performed the experiment, and revised the draft; Malago M edited the manuscript and provided financial support; Olde Damink SWM participated in the study design, interpreted the data, edited the manuscript, and provided financial support.

Supported by Citadel Capital Scholarship Foundation, Egypt; and Dr. Leslie Borthwick/Ms. Anita Holme, Charitable Research Fund East and North Herts NHS Trust Hertfordshire, United Kingdom
Correspondence to: Dipok Kumar Dhar, Senior Research Fellow, HPB and Liver transplantation surgery, Royal Free Hospital, University College London, 9th floor, London NW3 2PF, United Kingdom. d.dhar@ucl.ac.uk

Telephone: +44-207-7940500 Fax: +44-207-7940500

Received: June 1, 2011 Revised: September 2, 2011

Accepted: October 28, 2011

Published online: February 14, 2012

Abstract

AIM: To investigate a dual labeling technique, which would enable real-time monitoring of transplanted embryonic stem cell (ESC) kinetics, as well as long-term tracking.

METHODS: Liver damage was induced in C57/BL6 male mice ($n = 40$) by acetaminophen (APAP) 300 mg/kg administered intraperitoneally. Green fluorescence protein (GFP) positive C57/BL6 mouse ESCs were stained with the near-infrared fluorescent lipophilic tracer 1,1-dioctadecyl-3,3,3,3-tetramethylindotricarbocyanine iodide (DiR) immediately before transplantation

into the spleen. Each of the animals in the cell therapy group ($n = 20$) received 5×10^6 ESCs 4 h following treatment with APAP. The control group ($n = 20$) received the vehicle only. The distribution and dynamics of the cells were monitored in real-time with the IVIS Lumina-2 at 30 min post transplantation, then at 3, 12, 24, 48 and 72 h, and after one and 2 wk. Immunohistochemical examination of liver tissue was used to identify expression of GFP and albumin. Plasma alanine aminotransferase (ALT) was measured as an indication of liver damage.

RESULTS: DiR-stained ESCs were easily tracked with the IVIS using the indocyanine green filter due to its high background passband with minimal background autofluorescence. The transplanted cells were confined inside the spleen at 30 min post-transplantation, gradually moved into the splenic vein, and were detectable in parts of the liver at the 3 h time-point. Within 24 h of transplantation, homing of almost 90% of cells was confirmed in the liver. On day three, however, the DiR signal started to fade out, and *ex vivo* IVIS imaging of different organs allowed signal detection at time-points when the signal could not be detected by *in vivo* imaging, and confirmed that the highest photon emission was in the liver ($P < 0.0001$). At 2 wk, the DiR signal was no longer detectable *in vivo*; however, immunohistochemistry analysis of constitutively-expressed GFP was used to provide an insight into the distribution of the cells. GFP +ve cells were detected in tissue sections resembling hepatocytes and were dispersed throughout the hepatic parenchyma, with the presence of a larger number of GFP +ve cells incorporated within the sinusoidal endothelial lining. Very faint albumin expression was detected in the transplanted GFP +ve cells at 72 h; however at 2 wk, few cells that were positive for GFP were also strongly positive for albumin. There was a significant improvement in serum levels of ALT, albumin and bilirubin in both groups at 2 wk when compared with the 72 h time-point. In the cell therapy group, serum ALT was significantly ($P = 0.016$) lower and albumin ($P = 0.009$) was significantly higher when compared with the control group at the 2 wk time-point;

however there was no difference in mortality between the two groups.

CONCLUSION: Dual labeling is an easy to use and cheap method for longitudinal monitoring of distribution, survival and engraftment of transplanted cells, and could be used for cell therapy models.

© 2012 Baishideng. All rights reserved.

Key words: Cell transplantation; Cell tracking; Embryonic stem cells; Acute liver failure; Liver regeneration

Peer reviewers: Ekihiro Seki, MD, PhD, Department of Medicine, University of California San Diego, Leichag Biomedical Research Building, Rm. 349H, 9500 Gilman Drive MC#0702, La Jolla, CA 92093-0702, United States; Christopher Christophi, Professor and Head of The University of Melbourne Department of Surgery, Austin Hospital, Melbourne, 145 Studley Road, Victoria 3084, Australia; Maria Concepción Gutiérrez-Ruiz, PhD, Department of Health Sciences, Universidad Autónoma Metropolitana-Iztapalapa, DCBS, Av San Rafael Atlixco 186, Colonia Vicentina, DF 09340, México

Ezzat T, Dhar DK, Malago M, Olde Damink SWM. Dynamic tracking of stem cells in an acute liver failure model. *World J Gastroenterol* 2012; 18(6): 507-516 Available from: URL: <http://www.wjgnet.com/1007-9327/full/v18/i6/507.htm> DOI: <http://dx.doi.org/10.3748/wjg.v18.i6.507>

INTRODUCTION

Acute liver failure (ALF) is a life-threatening condition which often progresses rapidly to hepatic encephalopathy and multi-organ failure, leading to death within days. Viral hepatitis is the most common cause of ALF worldwide, with hepatitis B virus responsible for about 70% of cases^[1]. ALF following hepatic resections is rare, occurring in only 2.6% of patients. However, it produces significant morbidity and mortality^[2]. Another causative factor, which is more commonly encountered in the Western world, is acetaminophen (APAP) overdose, which leads to excessive production of its active metabolite N-acetyl-p-benzoquinone imine in the liver, causing depletion of the glutathione stores. This is ultimately followed by centrilobular hepatic necrosis and loss of functioning hepatocytes^[3]. APAP-induced liver toxicity is of significant importance because of its continued increase in incidence; it is currently the most common cause of ALF in the Western world^[4].

Several specific therapies have been designed to treat APAP-induced ALF. These have been in the form of drugs, such as N-acetyl cysteine being used to replenish glutathione stores in APAP-induced ALF^[5], or bioartificial devices to remove toxic metabolites and provide temporary support until native hepatocytes regenerate or as a bridge to liver transplantation (LTx)^[6]. LTx is the definitive therapy in patients not responding to conserva-

tive therapies which can only maintain the patients until a liver graft becomes available with moderate hypothermia as a bridge to LTx^[7,8]. Although the patient's survival after LTx for ALF is lower than that for chronic liver diseases, it is still highest among all other treatment options, with a long-term survival rate of about 70%^[9]. However, LTx may not always be feasible due to the severe shortage of donors. One alternative to LTx would be the use of pluripotent or multipotent cells to support the regeneration of the native liver.

So far, only a limited number of experimental studies used terminally differentiated hepatocytes to treat ALF with variable outcomes^[10,11]. Hepatocytes seem to be the optimum cell type to replenish the damaged liver; however, they need to be isolated from the donor livers. Also, they cannot be cultured for indefinite periods *in vitro*, and multiple hepatocyte transplantations may be required to achieve a satisfactory regenerative drive^[12].

These problems can be bypassed by the use of pluripotent or multipotent cells of different sources such as bone marrow, umbilical veins, fatty tissue or embryonic stem cells (ESCs). These cells have been used in the experimental set up to deliver genes to the liver in models with metabolic diseases^[13], and also used to treat chronic liver diseases such as cirrhosis^[14]. In the present study, we used undifferentiated ESCs in a mouse model of ALF to evaluate the cell kinetics. The ideal way of tracking transplanted cells used to repopulate damaged livers and improve their function remains to be elucidated. Optimizing cell therapies in patients would require an accurate, highly sensitive and non-invasive means to properly assess cell survival, biodistribution and fate in the same patient over time. Cell labeling offers the advantage of imaging distinct cell populations *in vivo* and investigating the efficacy of these therapies using non-invasive imaging techniques.

In this study, we wanted to evaluate a dual labeling technique, which enabled real-time monitoring of the kinetics of the transplanted ESCs as well as long-term tracking of the cells. A unique dual labeling of the cells was performed using a fluorescence dye and, for long-term tracking, a lentivirus mediated and constitutively expressed green fluorescence protein (GFP).

MATERIALS AND METHODS

Animals and experimental design

Forty male C57/BL6 mice (Charles River laboratories) at 5-6 wk of age with an average weight between 20-25 g were used for this study. All the surgical and experimental procedures were carried out according to the guidelines set by the University College London institutional procedures. All animals were acclimatized for 7 d prior to the experiments. The animals were allocated into 2 groups. Group 1 ($n = 20$) with cell therapy and group 2 ($n = 20$) with vehicle only. The group size was not powered for a mortality study. All animals received a single dose of APAP 300 mg/kg administered intraperitoneally^[15]. To ensure adequate dissolution, APAP was sonicated over-

Dynamic tracking of stem cells in an acute liver failure model				
Zero	4 h	24 h	72 h	2 wk
APAP	Cell Tx	Mortality	Sacrifice	Sacrifice
300 mg/kg (n = 40)				
Group 1	(n = 20)	(n = 9)	(n = 6)	(n = 5)
Group 2	(n = 20)	(n = 10)	(n = 5)	(n = 5)

Figure 1 Experimental animal design. Forty mice were treated with acetaminophen (APAP). The animals were then divided into 2 groups. The cell therapy group = Group 1 with cell transplantation and the control group = Group 2. During the first 24 h, 19/40 animals died due to the effect of APAP. Animals from both groups were then killed at 72 h when the signal started to decay and at two weeks when the signal could no longer be detected *in vivo*.

night in a water bath at 42 °C and the temperature was maintained until injection time. APAP administration was preceded by a subcutaneous injection of 10% dextrose in order to prevent mortality from severe hypoglycemia^[16]. The SC injection of 10% dextrose was repeated every 6 h during the first day of the experiment. At selected time points, the animals were killed by exsanguination (Figure 1). Time points were selected to have an optimal evaluation of ESC cell homing in organs using *ex vivo* imaging and for immunohistochemical (IHC) studies.

Embryonic stem cell line and culture conditions

Undifferentiated C57/BL6 ESCs constitutively expressing GFP (Millipore, Co Durham, United Kingdom) were maintained in the undifferentiated state using MilliTrace mouse ESC expansion medium (Millipore, Co Durham, United Kingdom), supplemented with 15% fetal bovine serum and leukemia inhibiting factor. Puromycin was added to the medium (0.5 µg/mL) for selective growth of GFP-positive cells. Cells were cultured on 0.1% gelatin coated T-75 cell culture flasks until 80% confluence was reached. The undifferentiated state of the ESCs was confirmed by alkaline phosphatase expression in more than 90% of the ESC colonies. Cell fixation was performed with 4% paraformaldehyde for 2 min followed by incubation with a mixture of fast red violet, naphthol AS-BI phosphate solution and water in a 2:1:1 ratio in a dark room for 15 min.

Dual labeling protocol

In order to achieve dual labeling of the GFP expressing ESCs for the purpose of *in vivo* tracking, the cells were labeled with the fluorescent lipophilic tracer 1,1-dioctadecyl-3,3,3,3-tetramethylindotricarbocyanine iodide (DiR) (Invitrogen Ltd, United Kingdom). The excitation/emission spectrum of DiR is in the near infrared range

(excitation 750 nm and emission 782 nm). After preparation of the stock solution, 5 mL of cell-labeling solution was directly applied to 1 mL cell suspension, mixed and incubated at 37 °C for 20 min. The labeled suspension was centrifuged at 1500 rpm for 5 min and the cell pellet was resuspended in warm fresh medium. This procedure was repeated twice to ensure complete removal of any unbound dye.

Cell preparation and transplantation

Following labeling with DiR, 5×10^6 cells were used per transplantation, which would be equivalent to approximately 7.5%-8% of the host liver hepatocytes^[17]. The cells were suspended in 100 µL of sterile phosphate buffer solution (PBS) in a syringe that was kept on ice until the time of transplantation. Cell transplantation was performed 4 h following treatment with APAP. Under adequate anesthesia and strict aseptic technique, a 1 cm incision was made in the left flank of the abdomen and the spleen was delivered outside the incision. The cells were injected into the spleen over a period of 5 min to prevent any loss of the cells due to overflow. Following injection, the needle was removed and fibrin glue applied to the injection site to prevent bleeding and cell loss. After confirming hemostasis, the spleen was replaced back into the abdominal cavity and the abdominal wall closed in a single layer. The same procedure was performed for the control group with PBS only.

Tracking of the transplanted cells

The mice were anesthetized with inhaled isoflurane and placed into the *In vivo* Imaging System (IVIS Lumina 2) chamber (Caliper Life Sciences, Cheshire, United Kingdom) and images were acquired using the CCD camera at 30 min post-transplantation, then at 3, 12, 24, 48 and 72 h, and after one and 2 wk. Following the sacrificing of the animals in groups at predetermined time periods, the spleen, liver, lung and kidney were placed inside the IVIS and images were acquired of the regions of interest to quantify the cell uptake in different organs. Three fluorescence filters [GFP, tricarboyanine 5.5 and indocyanine green (ICG)] were used to identify the filter with the least background autofluorescence. Data analysis was performed using the Living Image™ Software 3.0 (Caliper Life Sciences, Cheshire, United Kingdom).

Green fluorescence protein fluorescence

A Nikon fluorescence microscope (E501) was used for direct detection of GFP+ cells using the fluorescein isothiocyanate filter on frozen tissue sections.

Blood and tissue sampling

Following the culling the animals at 72 h and 2 wk, blood was collected by puncturing the suprahepatic vena cava, preserved on ice, then centrifuged to collect serum for further analysis of liver functions. Tissue samples of the liver and spleen were also collected and preserved for hematoxylin and eosin (HE) staining and IHC.

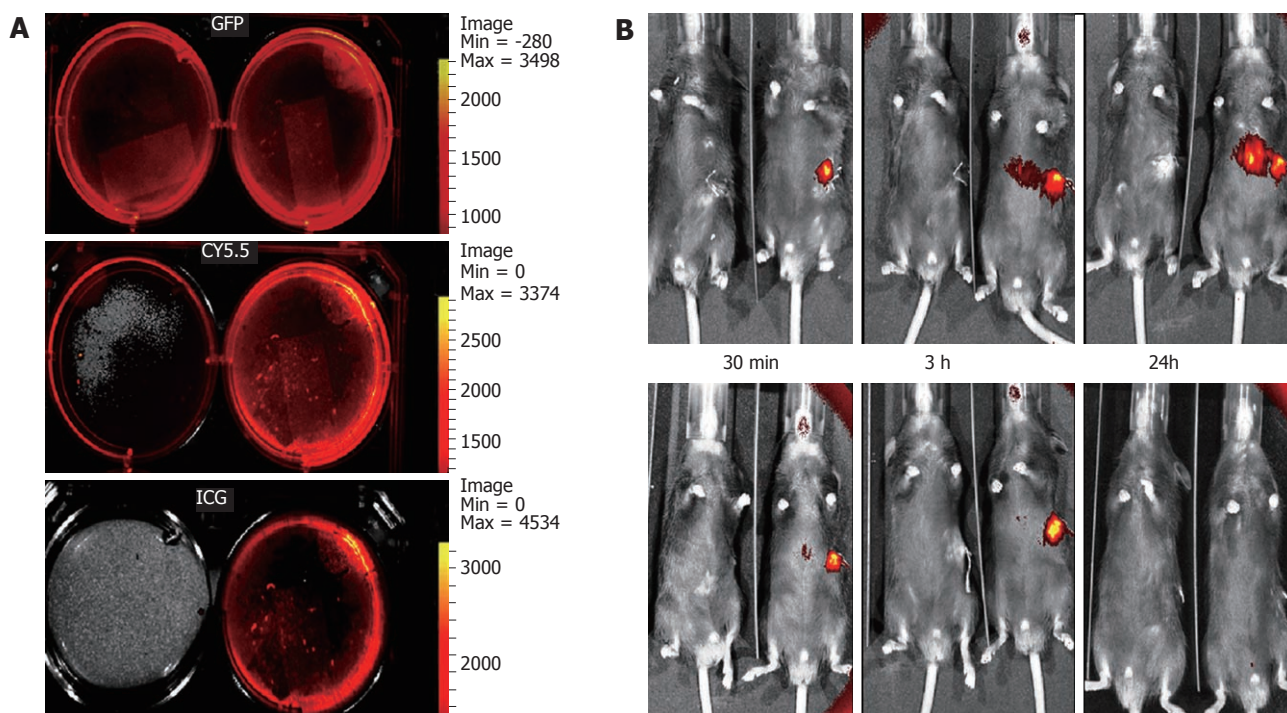


Figure 2 Labeling and tracking of the fluorescent embryonic stem cell following acetaminophen administration. IVIS images of green fluorescence protein (GFP) +ve cultured embryonic stem cells (ESCs) without 1,1-dioctadecyl-3,3,3,3-tetramethylindotricarbocyanine iodide (DiR) staining (LT) and with DiR staining (RT) showing background fluorescence using the GFP and tricarboyanine 5.5 filters, but not with the indocyanine green (ICG) filter (A). Images of a pair of mice (B), one from the cell therapy group-RT and the other from the control group-LT, were compared using IVIS. At 30 min following transplantation, a strong signal could only be detected from the spleen where the cells were injected. Between 3 and 24 h following the cell transplantation, the signal started to intensify between the spleen and the liver, which is most probably the splenic vein owing to its tortuous course. A strong signal was detected in the liver over 24 h post-transplantation, which faded out by the 72 h time-period. After one week, the signal could not be detected in the liver, but was still strong and was detectable over the spleen, which had completely disappeared by 2 wk.

Measurement of liver function tests

Measurement of hepatic enzyme and serum albumin levels were performed using the COBAS Integra 400 biochemistry analyzer (Roche) for measurement of plasma alanine aminotransferase (ALT), albumin, bilirubin and urea.

Immunohistochemistry

Sections of both the liver and spleen were preserved in 10% buffered formalin for HE staining and IHC studies. The IHC study was performed using the streptavidin ABC duet kit (Dako, Cambridgeshire, United Kingdom) on 5 μ m thick paraffin embedded tissue sections. Briefly, sections were dewaxed in xylene, rehydrated in graded alcohol and rinsed with PBS. Antigen retrieval was performed by heating in citrate buffer solution at 95 $^{\circ}$ C for 10 min. Endogenous peroxidase activity was blocked by incubating the slides with 3% hydrogen peroxide for 20 min. The sections were incubated at 4 $^{\circ}$ C overnight with primary antibodies; polyclonal rabbit anti-GFP (1:10, Millipore), and anti-albumin antibody (1:1000, Abcam). Streptavidin-peroxidase labeled secondary antibody was applied for 30 min at room temperature. Between steps, slides were rinsed with PBS solution. Color was developed with the chromogen 3,3'-diaminobenzidine (Dako, Cambridgeshire, United Kingdom), and counterstained with Mayer's hematoxylin solution.

Statistical analysis

Continuous variables were expressed as mean \pm SD. Differences were compared by *t*-test or Mann-Whitney *U* test as appropriate. For comparison of multiple groups, one-way ANOVA with Scheffe's *post-hoc* test was used. Differences in survival were analyzed by Kaplan Meier and a log rank test was used for significance. Statistical significance was taken as $P < 0.05$. All statistical analyses were done using the SPSS software for Windows 14.0 (SPSS, Inc., Chicago, IL).

RESULTS

In vivo detection of the transplanted cells

IVIS proved to be effective in precisely identifying the cells labeled with DiR in the liver and spleen at different time-points. This was possible only by using the ICG filter due to its high background passband of 665-695 nm with minimal background fluorescence (Figure 2A). At 30 min post-transplantation, the cells were confined inside the spleen and then gradually moved into the splenic vein and part of the liver at 3 h time point. By 24 h, the cells spread out over almost all areas of the liver and a residual signal was received over the spleen as well. The signal of DiR emitted from the liver faded out at 72 h. No signal could be detected in any other organs (Figure 2B).

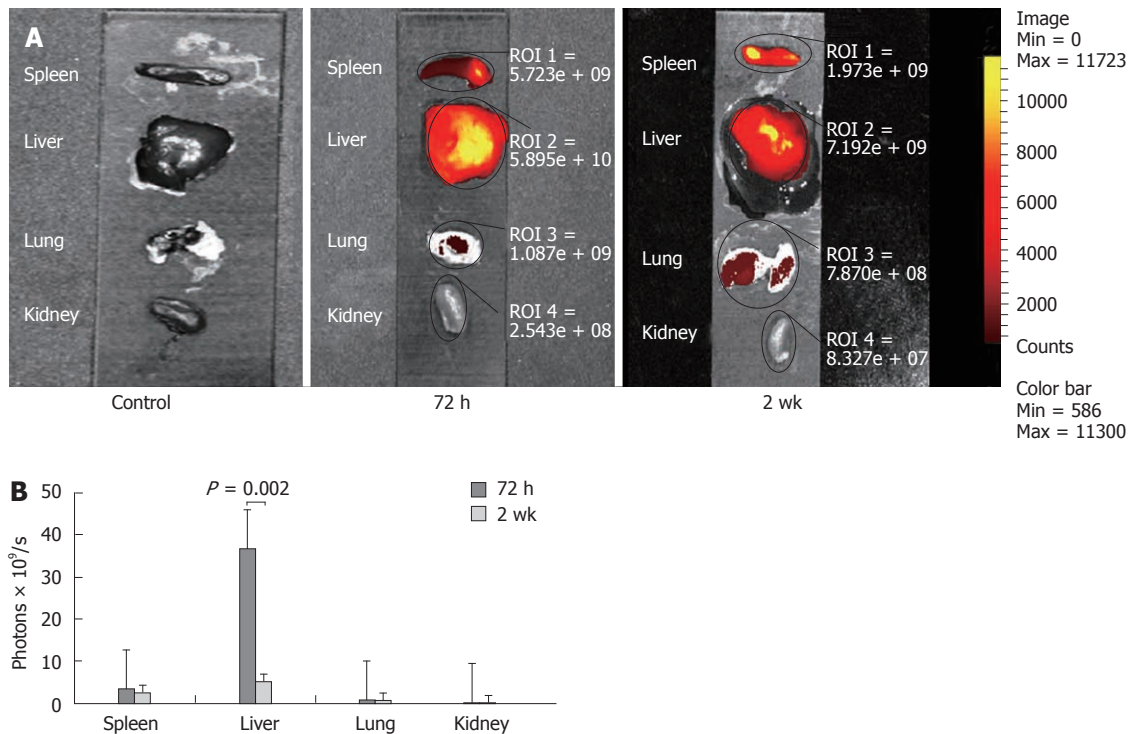


Figure 3 *Ex vivo* images showing the distribution of fluorescent cells in different organs as detected by the indocyanine green filter of the IVIS. A signal was detected at the site of injection in the spleen; however, the highest signal was noticed in the center of the liver at 72 h, which faded out by the 2 wk time-point. A weak fluorescent signal was also detected in the lungs at 72 h and 2 wk, but not seen in kidneys at any time-points (A). A graph showing the highest uptake of cells in the liver at all time-points with a significant drop at 2 wk (B).

Ex vivo imaging

A very clear fluorescent signal was detectable from both the liver and spleen when the organs were taken out and imaged directly with the IVIS. Eliminating the barrier effect of the anterior abdominal wall allowed signal detection at time-points when the signal could not be detected by *in vivo* imaging. Similar to *in vivo* imaging, the ICG filter was the most accurate filter to localize the cells with no autofluorescence from the organs. A weak signal was also detectable in the lungs and kidneys, in contrast to the *in vivo* imaging (Figure 3A). DiR uptake in the liver was significantly higher than the sum of uptake in all other organs at 72 h ($P < 0.0001$). At 2 wk, the amount of photons emitted from the liver decreased significantly from $3.67 \times 10^{10} \pm 1.7 \times 10^{10}$ photons/s at 72 h to $5.18 \times 10^9 \pm 1.58 \times 10^9$ ($P = 0.002$). However, in the liver, the emission was still significantly higher than the spleen ($P = 0.002$), lungs ($P < 0.0001$) and kidneys ($P < 0.0001$) (Figure 3B).

Engraftment of the transplanted cells in the liver

Frozen liver sections, using fluorescent microscopy, were studied to validate that the signal detected using the IVIS was definitely emitted from the engrafted cells and not from the released fluorescent dye DiR following cell death. GFP fluorescence from the transplanted cells was easily detectable by direct fluorescence microscopy at 72 h, however, it became much weaker at 2 wk and, therefore, we relied on IHC detection of GFP positive cells. At 72 h, discrete GFP +ve colonies were located under the liver

capsule and around the central veins (Figure 4A). GFP +ve cells were detected using IHC staining with anti-GFP +ve antibody. GFP +ve cells resembling hepatocytes were dispersed throughout the hepatic parenchyma with the presence of a larger number of GFP +ve cells incorporated within the sinusoidal endothelial lining (Figure 4E). GFP +ve cells could still be detected after 2 wk in the spleen, mainly around the central arteriole and the trabeculae (Figure 4F).

Effect of embryonic stem cell therapy on acetaminophen-induced liver injury

All mortality occurred during the first 24 h following APAP administration with 10/40 (25%) mice dying in the control group and 9/40 (22.5%) in the cell therapy group. According to the Kaplan Meier analysis, there was no significant difference in survival between the control and cell therapy groups ($P = 0.755$, log rank test). All animals surviving the initial 24 h lived until the time of sacrifice.

Liver damage was detected at 72 h, most prominent in the centrilobular regions with hepatocyte necrosis and secondary infiltration of inflammatory cells in both the cell therapy and control groups (Figure 4C and D). Improvement in liver histology was noticed both in both groups at 2 wk, with less inflammatory cell infiltration in the treatment group (Figure 4G and H).

In order to identify the nature of the transplanted cells, we stained with albumin antibody, which revealed very faint albumin expression in the GFP +ve cells at 72

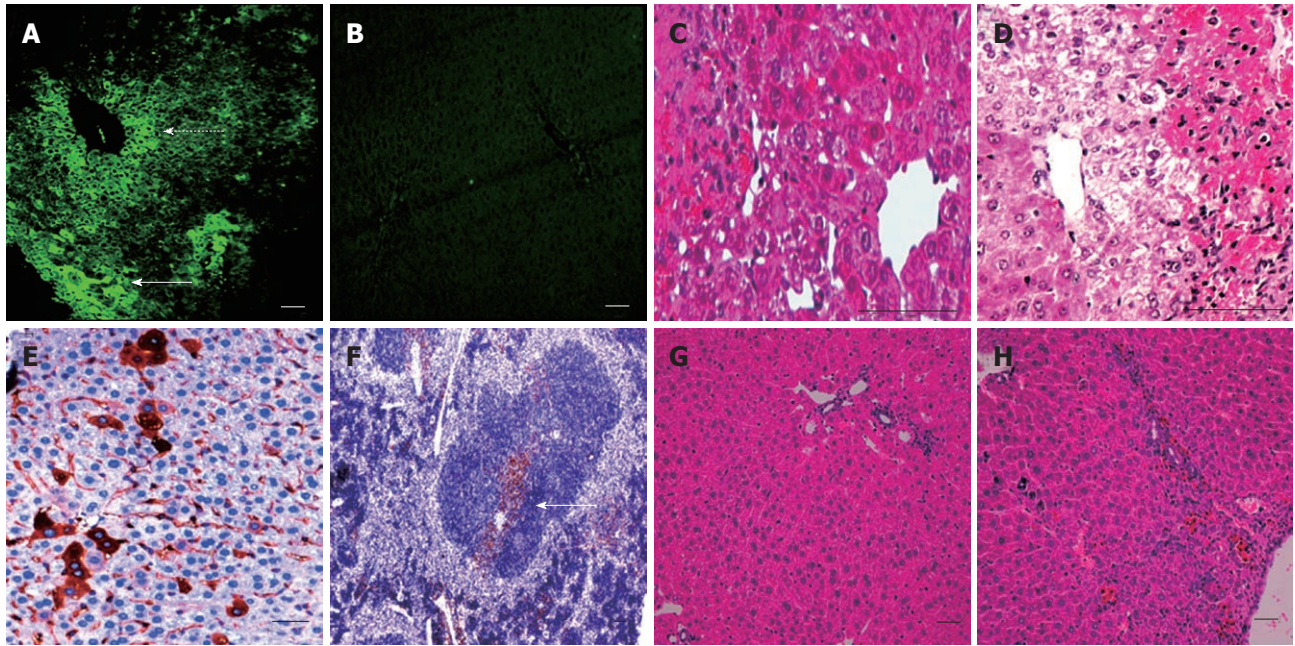


Figure 4 Embryonic stem cell liver engraftment following acetaminophen induced damage. A and B: Green fluorescence protein (GFP) +ve cells were present under the liver capsule (a-solid arrow) and around the central veins of the liver at 72 h, as seen under direct fluorescence (a-dashed arrow) with no fluorescence detected in the control group (B); C and D: The characteristic pattern of acetaminophen-induced liver damage after 72 h mainly affected the centrilobular portions of the liver, with marked damage of the pericentral hepatocytes in both the cell therapy and control groups, although pericentral vacuolation was more evident in the control group; E: At 2 wk, the GFP +ve cells could be detected using IHC in the hepatic parenchyma and within the sinusoidal lining; F: Localized colonies of GFP +ve cells were also detected in the spleen at 2 wk; G and H: After 2 wk the liver recovered in both groups, with the liver sections from the cell therapy group (G) showing less inflammatory cells and congestion than in the control group (H) (scale bar = 200 μ).

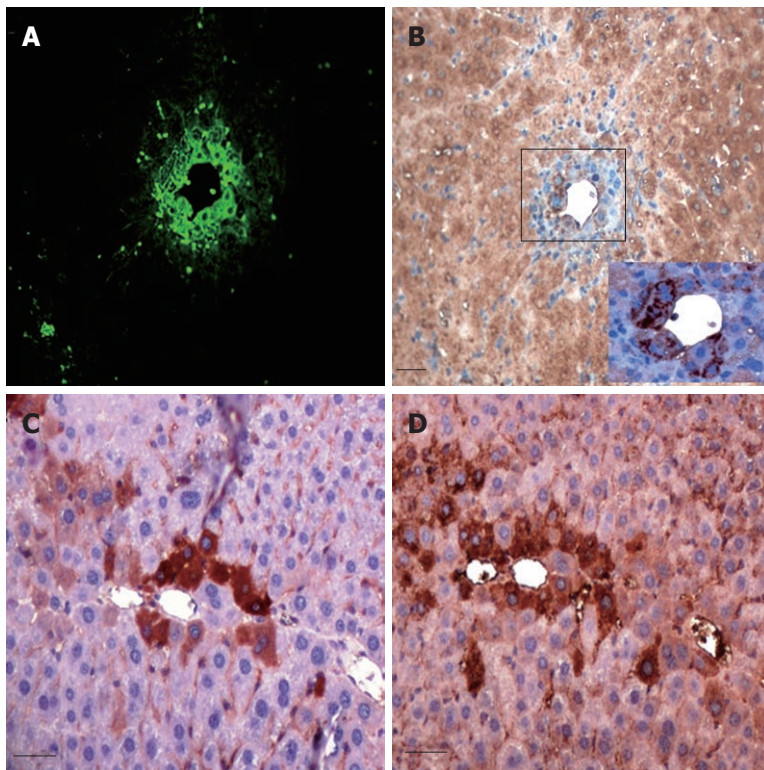


Figure 5 Serial sections examined for Green fluorescence protein and albumin expressions. Green fluorescence protein (GFP) +ve transplanted cells (A) showed very faint albumin expression at the cell periphery of dividing cells at 72 h (B), whereas areas stained with anti-GFP antibody (C) were positive for albumin (D) at 2 wk following cell therapy (scale bar = 100 μ).

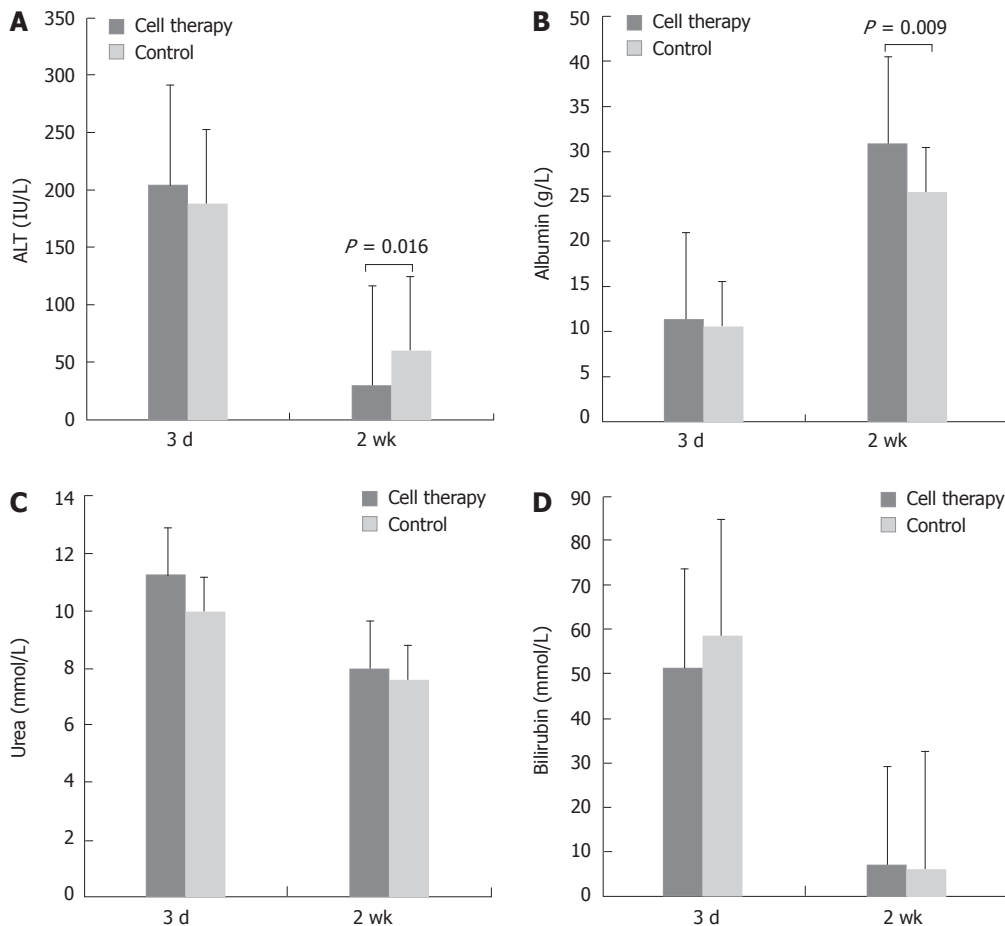


Figure 6 Serum levels of alanine aminotransferase, albumin, bilirubin and urea are shown ($n = 21$). A: The alanine aminotransferase (ALT) level significantly dropped in both groups at 2 wk when compared with the 72 h. When compared with the 72 h, there was a significant reduction in serum ALT level at 2 wk in the embryonic stem cell treatment group, but not in the control group; B: The albumin level also improved in both groups with the level being significantly higher in the cell therapy group when compared with the control group at 2 wk; C: The drop in urea levels was not significant in either group; D: Bilirubin levels dropped significantly from 72 h to 2 wk, with no significant differences between groups at similar time-points.

h (Figure 5A and B). However, when examined on serial sections, few cells that were positive for GFP were also strongly positive for albumin at 2 wk (Figure 5C and D).

There was a significant improvement in serum levels of ALT, albumin and bilirubin in both groups at 2 wk when compared with the 72 h time-point (Figure 6). Cell therapy itself had no effect on any of these parameters at the 72 h time point when compared with the control group. However, at 2 wk, serum ALT was significantly lower in the cell therapy group when compared to the control group (ALT: 29.58 ± 2.19 vs 60.38 ± 29.22 , cell therapy vs control group respectively, Mann U Whitney test $P = 0.016$, t -test $P = 0.07$) (Figure 6A). The serum albumin level was also significantly higher in the cell therapy group (Albumin: 30.8 ± 1.27 vs 25.54 ± 2.29 , cell therapy vs control group, respectively, $P = 0.009$) (Figure 6B). No significant changes occurred in serum bilirubin or urea levels between either group at 2 wk (Figure 6C and D).

DISCUSSION

In the present study we developed a novel model in which

we were able to monitor both the immediate and late kinetics of transplanted ESC cells. In this way, we were able to track the cells over days in real-time after the injection and had a better understanding about the dynamics of the cells in an experimental model of ALF without the need to sacrifice animals.

In the present model, we used APAP to induce ALF. So far, most of the existing animal models look into the role of cell therapy on liver regeneration following partial hepatectomy or hepatocellular damage induced by CCl₄^[18-20]. In these models, the roles of cell therapy were not studied in a pathophysiological milieu reciprocating the clinical scenario of ALF^[21]. For example, following liver resection, the liver bed reduces drastically and resection itself mobilizes the CD 133+ subset of cells from bone marrow into circulation, which may have played an independent role in liver regeneration^[22]. Moreover, CCl₄-induced liver damage builds up over time and does not produce a similar profound effect to that of ALF^[21]. In this study, we used an ALF model induced by APAP at a relatively moderate dose of 300 mg/kg, and transplanted the undifferentiated ESCs 4 h following induction of injury so that most of the APAP would have been me-

tabolized and would not interfere with ESCs survival^[15]. In order to track the cells *in vivo*, we used a reproducible imaging system for continuous real-time monitoring of the injected cells following transplantation. The IVIS is a relatively new optical imaging system that is being widely used in the fields of oncology and immunology, allowing non-invasive cell detection and migration^[23]. Near infrared dyes have been previously used for monitoring cells *in vivo* with improved quality of signal detection by increasing the contrast between the signal and the background, which is comprised mainly of water, oxyhemoglobin and deoxyhemoglobin^[24]. This has made it possible to track labeled cells located in deep-seated organs with minimal background fluorescence. To achieve that goal, we labeled the ESCs with a near infrared lipophilic tracer dye (DiR), which has the advantage of very low cell toxicity and laterally diffuses within the cell membrane, hence staining the whole cell. Very recently, Cho *et al.*^[25] used luciferase-transfected fetal hepatocyte cells for repopulating the liver in a monocrotaline-injected mice model and nicely showed the uptake of the cells by a CCD camera generated images. The advantages of the imaging we used in this study lies with the simplicity of the method. This technique is relatively cheap and easy to use without any necessity for genetic manipulation of the cells. There is also no necessity to inject any extra dye for visualization of the cells, which might interfere with body chemistry and prolong the anesthetic duration for the animals. The cells could be clearly seen migrating from the spleen to the liver (Figure 2). The signal intensity in the liver was highest between the second and third days post-transplantation, possibly because cell proliferation is highest at that time^[26]. A rapid drop in the signal intensity was noticed after the third day and continued to fade until it completely disappeared at 2 wk post-transplantation. Similar to the DiR dye we used, the signal from firefly luciferase also dropped on day 10 following hepatocyte transplantation^[25]. However, visualization and quantification of the transplanted cells was still possible at 2 wk by DiR imaging when the organs were extracted and imaged directly under the IVIS.

Since the ESCs were transfected with GFP, it was possible to observe the distribution of the transplanted cells on tissue sections directly under the fluorescent microscope or by immunohistochemistry using the anti-GFP antibody. Engraftment of the ESCs was confirmed on liver tissue sections in the post-transplantation period by direct visualization of GFP +ve cells, which appeared in the close vicinity of the central veins where the main brunt of the damage had occurred. The homed pericentral cells subsequently proliferated and spread throughout the liver parenchyma. The mechanism through which the ESCs integrate into the liver plate depends primarily on the disruption of the sinusoidal endothelial cells^[27]. Although APAP overdose characteristically affects the centrilobular regions of the liver, causing extensive necrosis, there is also a direct toxic effect on the sinusoidal endothelial cells through glutathione depletion^[28] and thus this

may have played a role in the uptake of cells into the liver parenchyma, particularly since GFP +ve cells were also detected in the sinusoidal endothelial lining at 2 wk.

ESC transplantation did not improve either survival or liver functions at 72 h. At 2 wk some transplanted cells expressed albumin and morphologically resembled hepatocytes. There was an increase in serum albumin production at 2 wk in the cell therapy group when compared to the control group. It is unlikely that the differentiation of transplanted cells into hepatocytes could explain the improved liver functions at 2 wk in the cell therapy group, since the cells were few and we did not perform additional studies to confirm differentiation as this was not the purpose of the study. The paracrine effect of the transplanted cells, rather than direct differentiation, seems to be a more possible cause of improved liver functions. Mesenchymal stem cell conditioned medium has been shown to improve liver functions following induction of ALF in rats^[29]. Proteins released from human undifferentiated ESCs were also shown to improve cardiomyocytes function^[30].

ESC therapy has been riddled with several problems including allogenic rejection, ethical concerns and, most importantly, chances of malignant transformation of ESCs. Although Moriya *et al.*^[31] did not detect any teratoma formation following transplantation of undifferentiated ESCs in a liver cirrhosis model in mice; the transformation of undifferentiated ESCs into teratomas is very likely after a period of time. We used undifferentiated ESCs in this study to develop a suitable model to study the kinetics of transplanted cells in ALF; however, to study the therapeutic effect of ESCs in ALF, ideally we should have used differentiated ESCs, pluripotent stem cells or primary hepatocytes. Differentiation of ESCs *in vitro* into hepatocytes has been extensively studied by several groups and could be achieved by formation of embryoid bodies^[32], or directly by adding growth factors to the ESCs in monolayer cultures^[33]. However, full maturation of hepatocytes is not complete without the influence of the intrinsic environment^[34]. Several studies have been conducted to simulate the inductive microenvironment *in vitro*, either through co-cultures with hepatocytes^[35] or using conditioned media in *in vitro* cultures^[36].

We conclude that serial longitudinal tracking of transplanted cells in a mouse model of ALF is possible using IVIS and that dual labeling would allow for both immediate and long-term tracking of the transplanted cells, which would in turn allow us to better understand their differentiation and fate.

COMMENTS

Background

Acute liver failure is a life-threatening condition. Several therapies have been designed to treat this condition with mixed results. Stem cells represent a promising therapeutic modality; however, in order to optimize cell therapy, it would be necessary to develop an accurate cell tracking method.

Research frontiers

We developed a novel imaging system for stem cell tracking using a dual

labeling fluorescent protocol. It was possible to track the cell dynamics *in vivo* without killing the animals, giving an insight into the cell biodistribution in different organs. This would allow real-time monitoring in the early phase following development of acute liver failure which would be very beneficial in optimizing cell therapy.

Innovations and breakthroughs

Other methods of cell monitoring rely either on early or late tracking of cells. Through dual labeling we could take advantage of the near infrared cell label, which is very efficient in localizing the cells *in vivo*, but has a short half-life. The authors could then track the green fluorescence protein label, which is not efficient for *in vivo* cell tracking, but could be used for localizing the cells in tissue sections either directly or indirectly even after a long period of time.

Application

Understanding cell dynamics in the acute phase of liver failure would allow for the optimizing of cell therapies according to the time-points when the cells engraft in the liver and could then serve as an alternative therapeutic option to liver transplantation.

Peer review

This is an interesting study about some non-invasive methods for tracking stem cells to evaluate the cell engraftment following acute liver failure by acetaminophen. The authors developed an interesting and novel model for *in vivo* tracking of embryonic stem cells, based in stained green fluorescence protein embryonic stem cells with the IVIS Lumina-2. Immunohistochemistry for albumin and green fluorescence protein were used to confirm liver embryonic stem cell nesting.

REFERENCES

- Lee WM. Etiologies of acute liver failure. *Semin Liver Dis* 2008; **28**: 142-152
- van den Broek MA, van Dam RM, Malagó M, Dejong CH, van Breukelen GJ, Olde Damink SW. Feasibility of randomized controlled trials in liver surgery using surgery-related mortality or morbidity as endpoint. *Br J Surg* 2009; **96**: 1005-1014
- Martin-Murphy BV, Holt MP, Ju C. The role of damage associated molecular pattern molecules in acetaminophen-induced liver injury in mice. *Toxicol Lett* 2010; **192**: 387-394
- Larson AM, Polson J, Fontana RJ, Davern TJ, Lalani E, Hynan LS, Reisch JS, Schiødt FV, Ostapowicz G, Shakil AO, Lee WM. Acetaminophen-induced acute liver failure: results of a United States multicenter, prospective study. *Hepatology* 2005; **42**: 1364-1372
- Heard KJ. Acetylcysteine for acetaminophen poisoning. *N Engl J Med* 2008; **359**: 285-292
- Sen S, Williams R, Jalan R. Emerging indications for albumin dialysis. *Am J Gastroenterol* 2005; **100**: 468-475
- Jalan R, Olde Damink SW, Deutz NE, Lee A, Hayes PC. Moderate hypothermia for uncontrolled intracranial hypertension in acute liver failure. *Lancet* 1999; **354**: 1164-1168
- Jalan R, Olde Damink SW, Deutz NE, Hayes PC, Lee A. Moderate hypothermia in patients with acute liver failure and uncontrolled intracranial hypertension. *Gastroenterology* 2004; **127**: 1338-1346
- Farmer DG, Anselmo DM, Ghobrial RM, Yersiz H, McDiarmid SV, Cao C, Weaver M, Figueroa J, Khan K, Vargas J, Saab S, Han S, Durazo F, Goldstein L, Holt C, Busuttill RW. Liver transplantation for fulminant hepatic failure: experience with more than 200 patients over a 17-year period. *Ann Surg* 2003; **237**: 666-675; discussion 675-676
- Mei J, Sgroi A, Mai G, Baertschiger R, Gonelle-Gispert C, Serre-Beinier V, Morel P, Bühler LH. Improved survival of fulminant liver failure by transplantation of microencapsulated cryopreserved porcine hepatocytes in mice. *Cell Transplant* 2009; **18**: 101-110
- Riordan SM, Williams R. Acute liver failure: targeted artificial and hepatocyte-based support of liver regeneration and reversal of multiorgan failure. *J Hepatol* 2000; **32**: 63-76
- Rajvanshi P, Kerr A, Bhargava KK, Burk RD, Gupta S. Efficacy and safety of repeated hepatocyte transplantation for significant liver repopulation in rodents. *Gastroenterology* 1996; **111**: 1092-1102
- Eavri R, Lorberboum-Galski H. A novel approach for enzyme replacement therapy. The use of phenylalanine hydroxylase-based fusion proteins for the treatment of phenylketonuria. *J Biol Chem* 2007; **282**: 23402-23409
- Terai S, Sakaida I. Autologous bone marrow cell infusion therapy for liver cirrhosis patients. *J Hepatobiliary Pancreat Sci* 2011; **18**: 23-25
- Saito C, Zwingmann C, Jaeschke H. Novel mechanisms of protection against acetaminophen hepatotoxicity in mice by glutathione and N-acetylcysteine. *Hepatology* 2010; **51**: 246-254
- Scorticati C, Prestifilippo JP, Eizayaga FX, Castro JL, Romay S, Fernández MA, Lemberg A, Perazzo JC. Hyperammonemia, brain edema and blood-brain barrier alterations in prehepatic portal hypertensive rats and paracetamol intoxication. *World J Gastroenterol* 2004; **10**: 1321-1324
- Ponder KP, Gupta S, Leland F, Darlington G, Finegold M, DeMayo J, Ledley FD, Chowdhury JR, Woo SL. Mouse hepatocytes migrate to liver parenchyma and function indefinitely after intrasplenic transplantation. *Proc Natl Acad Sci USA* 1991; **88**: 1217-1221
- Liu ZC, Chang TM. Transdifferentiation of bioencapsulated bone marrow cells into hepatocyte-like cells in the 90% hepatectomized rat model. *Liver Transpl* 2006; **12**: 566-572
- Gao Y, Mu N, Xu XP, Wang Y. Porcine acute liver failure model established by two-phase surgery and treated with hollow fiber bioartificial liver support system. *World J Gastroenterol* 2005; **11**: 5468-5474
- Mark AL, Sun Z, Warren DS, Lonze BE, Knabel MK, Melville Williams GM, Locke JE, Montgomery RA, Cameron AM. Stem cell mobilization is life saving in an animal model of acute liver failure. *Ann Surg* 2010; **252**: 591-596
- Tuñón MJ, Alvarez M, Culebras JM, González-Gallego J. An overview of animal models for investigating the pathogenesis and therapeutic strategies in acute hepatic failure. *World J Gastroenterol* 2009; **15**: 3086-3098
- Gehling UM, Willems M, Dandri M, Petersen J, Berna M, Thill M, Wulf T, Müller L, Pollok JM, Schlagner K, Faltz C, Hossfeld DK, Rogiers X. Partial hepatectomy induces mobilization of a unique population of haematopoietic progenitor cells in human healthy liver donors. *J Hepatol* 2005; **43**: 845-853
- Eisenblätter M, Ehrchen J, Varga G, Sunderkötter C, Heindel W, Roth J, Bremer C, Wall A. In vivo optical imaging of cellular inflammatory response in granuloma formation using fluorescence-labeled macrophages. *J Nucl Med* 2009; **50**: 1676-1682
- Weissleder R. A clearer vision for in vivo imaging. *Nat Biotechnol* 2001; **19**: 316-317
- Choi MS, Catana AM, Wu J, Kim YS, Yoon SJ, Borowsky AD, Gambhir SS, Gupta S, Zern MA. Use of bioluminescent imaging to assay the transplantation of immortalized human fetal hepatocytes into mice. *Cell Transplant* 2008; **17**: 899-909
- Garcea G, Maddern GJ. Liver failure after major hepatic resection. *J Hepatobiliary Pancreat Surg* 2009; **16**: 145-155
- Gupta S, Rajvanshi P, Sokhi R, Slehria S, Yam A, Kerr A, Novikoff PM. Entry and integration of transplanted hepatocytes in rat liver plates occur by disruption of hepatic sinusoidal endothelium. *Hepatology* 1999; **29**: 509-519
- DeLeve LD, Wang X, Kaplowitz N, Shulman HM, Bart JA, van der Hoek A. Sinusoidal endothelial cells as a target for acetaminophen toxicity. Direct action versus requirement for hepatocyte activation in different mouse strains. *Biochem Pharmacol* 1997; **53**: 1339-1345
- van Poll D, Parekkadan B, Cho CH, Berthiaume F, Nahmias Y, Tilles AW, Yarmush ML. Mesenchymal stem cell-derived molecules directly modulate hepatocellular death and regeneration in vitro and in vivo. *Hepatology* 2008; **47**: 1634-1643
- LaFramboise WA, Petrosko P, Krill-Burger JM, Morris DR, McCoy AR, Scalise D, Malehorn DE, Guthrie RD, Becich MJ,

- Dhir R. Proteins secreted by embryonic stem cells activate cardiomyocytes through ligand binding pathways. *J Proteomics* 2010; **73**: 992-1003
- 31 **Moriya K**, Yoshikawa M, Ouji Y, Saito K, Nishiofuku M, Matsuda R, Ishizaka S, Fukui H. Embryonic stem cells reduce liver fibrosis in CCl4-treated mice. *Int J Exp Pathol* 2008; **89**: 401-409
- 32 **Chinzei R**, Tanaka Y, Shimizu-Saito K, Hara Y, Kakinuma S, Watanabe M, Teramoto K, Arii S, Takase K, Sato C, Terada N, Teraoka H. Embryoid-body cells derived from a mouse embryonic stem cell line show differentiation into functional hepatocytes. *Hepatology* 2002; **36**: 22-29
- 33 **Hamazaki T**, Iiboshi Y, Oka M, Papst PJ, Meacham AM, Zon LI, Terada N. Hepatic maturation in differentiating embryonic stem cells in vitro. *FEBS Lett* 2001; **497**: 15-19
- 34 **Imamura T**, Cui L, Teng R, Johkura K, Okouchi Y, Asanuma K, Ogiwara N, Sasaki K. Embryonic stem cell-derived embryoid bodies in three-dimensional culture system form hepatocyte-like cells in vitro and in vivo. *Tissue Eng*; **10**: 1716-1724
- 35 **Novik EI**, Barminko J, Maguire TJ, Sharma N, Wallenstein EJ, Schloss RS, Yarmush ML. Augmentation of EB-directed hepatocyte-specific function via collagen sandwich and SNAP. *Biotechnol Prog*; **24**: 1132-1141
- 36 **Min J**, Shang CZ, Chen YJ, Zhang L, Liu L, Deng XG, Yang M, Chen DP, Cao J, Song EW, Chen JS. Selective enrichment of hepatocytes from mouse embryonic stem cells with a culture system containing cholestatic serum. *Acta Pharmacol Sin* 2007; **28**: 1931-1937

S- Editor Lv S L- Editor Rutherford A E- Editor Xiong L